

# Modelling analysis of antenna structures for mobile communication devices considering AWS downlink band range

Liyao Wang<sup>1</sup>, Lusheng Yang<sup>2</sup>

<sup>1</sup>College of Engineering, Yanbian University, Yanji, 133000, China

<sup>2</sup>College of Computer and Communication, Lanzhou University of Technology, Lanzhou, 730050, China

**Abstract:** Modern mobile communication technology and mobile phone business are developing at a rapid pace, the mobile phone is constantly being updated. PIFA antennas are widely used in mobile communication terminal devices such as mobile phones for their small size, lightweight, low profile and other advantages. The research on using PIFA antenna to achieve multi-band, miniaturization, broadband and other functional characteristics has made certain achievements. In this paper, the structure of the PIFA antenna itself is optimized with the objectives of high accuracy, high integration and economy, the real geometry of the PIFA antenna is modelled through simulation, and the frequency range of the antenna tuning applicable to the AWS band is limited, the spatial electric field distribution, the far-field radiation gain characteristics and the S-parameter characteristics of the antenna are explored under the influence of different parameters, and finally, its wireless communication capability is analysed and summarised and It is then compared with the operational specifications of modern portable communication devices.

**Keywords:** PIFA, antenna structure, finite element method, space electric field, gain S-parameters

## 1. Introduction

Modern mobile communication technology is developing at a rapid pace. the mobile phone business is developing more and more rapidly, the mobile phone continuously receives updates, getting lighter and easier to carry around and functional. The built-in antenna needs to be able to function across a wider range of frequencies and in increasingly compact dimensions. And at the same time the performance cannot be affected [1]. Modern mobile phone antenna design relies heavily on the utilization of Planar inverted F antenna (PIFA) [2]. Traditional monopole antennas are not stable and difficult to guarantee because of their high environmental requirements and susceptibility to interference from the surrounding environment. And in resonance is difficult to impedance matching, and it is so hard to ensure that a certain level of radiation efficiency is achieved. Analysed in terms of miniaturisation, not only is its electrical size large, but it is also so hard to combine multiple monopole antennas. From the price point of view, if monopole antennas want to achieve the function of applying multi-band, it is relatively difficult, the space required becomes bigger, and the capital investment becomes bigger. Compared to monopole antennas, PIFA antennas evolved from microstrip antennas have a smaller electrical size and are easy to make into laminated sheets, which makes radiation greatly enhanced and radiation efficiency greatly improved. Therefore, PIFA antennas are more suitable for achieving multi-band, miniaturisation and broadband functions of antennas, and they are used extensively in the industry.

To address the increasing demand for built-in antennas for the applicable frequency bands, some scholars have earlier proposed the idea that the antenna multi-band operation can be achieved by using the method of slotting on the patch to achieve the function. In the meantime, the process of building and testing a prototype and conducting simulated trials of open L-slot and open U-slot have been carried out. After experiments, it has been proven that two models allow for dual-band functionality, but the return loss and voltage VSWR of the antenna are marginally higher, and need continued enhancement and optimisation [3]. Certain academics have made significant progress in their examination of theoretical concepts. The impact of five variables was examined through the utilization of a finite element algorithm in the literature [4] which are on the antenna performance: radiation plane height, ground plane width, ground plane length, horizontal distance of the short circuit point from the feed point, and short circuit plane width. And depending on the influence of the parameters on performance, the research designed a three-band PIFA antenna, which achieved breakthroughs and advancements. Subsequently, there has

been additional investigation and improvement on this issue by many scholars. One of the models proposed in the literature [5] is the construction of a pair of identical curving notches loaded on the radiator of the topmost stratum of the PIFA antenna. A dual-band slotted PIFA antenna in a triangular configuration with directional radiation characteristics is formed. This enables the built-in antenna to be used for both high and low frequency bands. In the literature [6] a method is given to handle the using a multi-branching technique. This gives different lengths starting at the source, the signal travels through the primary junction and splits into the main and auxiliary pathways. This results in resonance at two frequency points, enabling adaptation to two distinct wavelengths of electromagnetic radiation, while decreasing the width of the WLAN terminal to meet the need for miniaturisation. The literature [7] also devised a clever plan utilizing the manipulation of radio wave frequencies through antenna reconfiguration techniques, which refers to the incorporation of variable-state components in the antenna circuit. And through altering the configuration of these elements, the operating frequency of the antenna is changed to make the antenna suitable for multi-band functions. The scholar uses the capacitance rating of the adjustable capacitor in the circuit to change the working frequency. Through experimental simulation, it can be seen that the capacitance value affects the low frequency range of the antenna. However, capacitance variations do not significantly impact the high-frequency range of the antenna. This approach displays imperfections that are apparent. To this end, Professor Liu Zewen, Institute of Microelectronics at Tsinghua University, proposed to use the TIC method to use the tic method to be adjusted and dual -frequency PIFA antenna, i.e. the tunable inductance and capacitance are used to achieve a tunable dual-band antenna performance. The method consists of a two-stage tunable circuit, with the first stage consisting of a tunable capacitor and the second stage consisting of a tunable capacitor and a tunable inductor. Through simulations, the result proves that the tic method that uses the TIC method is not only applicable to the low -frequency band, but the S value of the high frequency band is also greatly reduced [8]. Several contemporary techniques for multi-band mobile phone antennas are currently popular which have been introduced in the literature [9], including coupled-feed, reconfigurable and multi-radiation branching techniques. However, it is still facing problems such as the influence of neighboring digital devices and signal attenuation. In addition to the need to address the increasing demand for built-in antennas in the applicable frequency bands, the issue of miniaturisation also needs to be addressed. Some scholars, to realize the miniaturization of the antenna and expand the impedance bandwidth problem, build the model of the PIFA antenna radiation piece and the ground loaded with an inverted L-shaped step, after conducting electromagnetic simulations, optimizing parameters, and performing physical processing tests, the results of the tests align with the predicted outcomes from the simulations. The broadening of the range of impedance frequencies are achieved. Achieving favorable radiation properties. As a result, the practicality of reducing the size of antennas while maintaining a wide range of frequencies has been confirmed [10]. In [11], a bending and folding method is proposed to miniaturize the PIFA antenna. Specifically, the PIFA antenna is placed vertically and the short road surface of the drive unit and the parasite unit is overlapped to reduce the size of the antenna in the resonant direction. So as to achieve smallization of antenna. A broadband single-polarised microstrip antenna is described in the literature [12]. It is designed with two "L"-shaped probes and a "T"-shaped printed board arrangement, and the simulated experiments demonstrate that the bandwidth is increased and the feasibility of broadband is verified.

In summary, the use of PIFA antennas to achieve multi-band, miniaturisation and broadband functionalities has already achieved certain results, however, there is still some room for optimising the design of antenna structures for mobile communication devices to achieve high accuracy, high integration and economic goals. Therefore, this paper investigates the problem of optimising the tuning performance of PIFA antennas for multi-band applications. Firstly, the real geometric structure of PIFA is modelled with mobile communication equipment as the research object, and the antenna tuning is adopted for the frequency range of the AWS band to investigate the S-parameters, impedance matching characteristics, spatial electric field distribution and far-field radiation gain characteristics under the influence of different parameters, and the far-field radiation direction diagram is simulated to analyse the capability of wireless communication to realise the PIFA structure for AWS band frequency and antenna tuning characteristics to satisfy the operational needs of modern mobile communication devices.

## **2. Fundamental principles**

### ***2.1 Basic Principles of antenna structures in wireless network communication systems***

Wireless communication is a form of communication that uses the properties of electromagnetic wave signals that travel through free space to exchange information. And wireless communication achieved on

the move is called mobile communication, which must be transmitted using radio waves. An antenna is a device that transmits or receives electromagnetic waves in a radio system. Its main functions are: to act as an energy converter to achieve the conversion of guided electromagnetic and radio waves; to distribute energy spatially so that it is directional; and to radiate or receive a specified polarisation wave, i.e. to form the required polarisation. The antenna consists mainly of the radiation unit, the reflector plate, the power distribution network and the package protection. An early IFA antenna that is widely used in modern mobile phone antenna designs is shown in Fig.1. The PIFA antenna is formed by flattening the horizontal part of the IFA antenna.

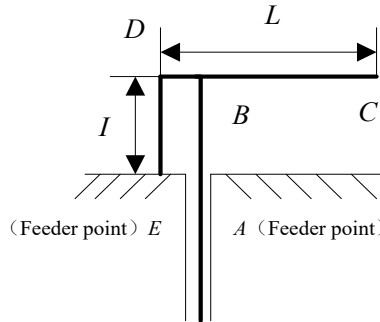


Figure 1: IFA antenna

Antennas can both radiate and receive radio waves, so the analysis and design of antennas are based on electromagnetic field theory. Maxwell's system of equations is a universal set of equations applicable to all macroscopic electromagnetic fields, which was developed after summarising previous practical investigations and theoretical studies on electromagnetic fields. The theory of electromagnetic fields obtained from Maxwell's equations is the basis for solving antenna-related problems and other electromagnetic field problems. The differential form of Maxwell's system of equations is as follows:

$$\begin{cases} \nabla \times \mathbf{E} = -\frac{\partial \mathbf{B}}{\partial t} \\ \nabla \times \mathbf{H} = \mathbf{J} + \frac{\partial \mathbf{D}}{\partial t} \\ \nabla \cdot \mathbf{D} = \rho_v \\ \nabla \cdot \mathbf{B} = 0 \end{cases} \quad (1)$$

Where  $\mathbf{E}$  is the electric field strength in  $V/m$ ;  $\mathbf{H}$  is the magnetic field strength in  $A/m$ ;  $\mathbf{D}$  is the electric flux density in  $C/m^2$ ;  $\mathbf{B}$  is the magnetic flux density in  $Wb/m^2 = V \cdot S/m^2 = T$ ;  $\mathbf{J}$  is the bulk current density in  $A/m^2$ ;  $\rho_v$  is the bulk charge density in  $C/m^3$ .

Scattering theorem: The score of the scattered scale of the method of any vector field on the closed surface is equal to the volume score of its scattered degree surrounded by the closed surface. The application of the scattering theorem allows one to relate the triple integral within a volume of space to the double integral on its surface. That is, the volume is  $v$  divided into several small units of infinitesimal volume. Rotation, i.e. the line integral over the perimeter of a unit area. There is a surface  $S$ , divided into several small area units of area  $\Delta S$ , and on each area unit, the degree of rotation is applied. Since the common boundary of every two neighbouring area units  $\Delta S$  is in opposite directions, their integral values can cancel, so that only the integral over the perimeter of the surface  $S$  is valid This is Stokes' theorem. Applying Stokes' theorem, the integral form of Maxwell's system of equations can be obtained.

### 2.1.1 Fluctuation Equations for Electric and magnetic fields

Let the bulk density of free charges in a region be zero and the medium be homogeneous, linear and isotropic; under such conditions, Maxwell's set of equations takes different forms. The fluctuation equations for the electric and magnetic fields can be found using the dispersion theorem and the rotational degree.

$$\begin{cases} \left( \nabla^2 - \sigma\mu \frac{\partial}{\partial t} - \varepsilon\mu \frac{\partial^2}{\partial t^2} \right) \mathbf{E} = 0 \\ \left( \nabla^2 - \sigma\mu \frac{\partial}{\partial t} - \varepsilon\mu \frac{\partial^2}{\partial t^2} \right) \mathbf{H} = 0 \end{cases} \quad (2)$$

Where the dielectric constant is  $\epsilon$ , the magnetic permeability is  $\mu$  and the electrical conductivity is  $\sigma$ .

To simplify the difficulty of setting boundary conditions, we use the ideal electric conductor condition and set the relative permittivity  $\epsilon_r$ . Because the signal is time-harmonic, the Helmholtz equation is used to solve for the electric field vector at any location in the geometric structure, as shown in equation (3). The far-field domain can also be calculated to obtain the far-field distribution at infinity, as shown in equation (4). Fig.2 shows a simulation of a mobile phone antenna radiating and receiving radio waves.

$$\nabla \times \mu^{-1} (\nabla \times \mathbf{E}) - k^2 \epsilon_r \mathbf{E} = 0 \quad (3)$$

$$E_{far} = -\frac{jk}{4\pi} r_0 \times \int [n \times E - \eta r_0 \times (n \times H)] \exp(jkr r_0) dS \quad (4)$$

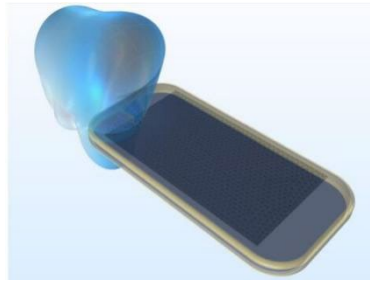


*Figure 2: Simulation diagram of mobile phone antenna radiation and received radio waves*

## 2.2 Factors influencing antenna performance

To measure the antenna to achieve the conversion of guided electromagnetic and radio waves, the spatial distribution of energy, the formation of the required polarization and other functions, there are radiation efficiency, beam width, directional coefficient, gain, input impedance, polarization and bandwidth and other antenna electrical parameters. These antenna electrical parameters directly determine the performance index of the whole system. One of the directional coefficients is one of the main electrical parameters, used to quantitatively describe the antenna's directional strength, directional coefficient  $D$  is defined as the antenna in the direction of maximum radiation in the far area of a point of power density and radiation power of the same directional antenna in the same point of power density ratio. Antenna gain is defined as the antenna in the maximum radiation direction in the far area of a point of power density and input power of the same non-directional in the same point of the power density ratio. The input impedance of the antenna is defined as the impedance presented by the antenna at its input, which is an electrical parameter reflecting the characteristics of the antenna circuit. Voltage standing wave ratio (VSWR) is defined as the transmission line adjacent to the wave web voltage amplitude and the ratio of the voltage amplitude of the wave section, said the feed line standing wave state. The bandwidth of the antenna is defined as the frequency range of the antenna's electrical parameters within the tolerance range. The polarization of the antenna is defined as the polarization of the electromagnetic wave radiated by the antenna in a given direction.

The following are the factors influencing antenna performance:

### 2.2.1 The correlation between antenna efficiency and radiation resistance

Due to the antenna itself and the consumption of media, support structure, and grounding device loss, the input antenna power cannot be 100% of the antenna radiation power. The antenna's effectiveness is determined by the proportion of power radiated by the antenna to the power supplied to it. Radiation resistance is an important indicator for measuring antenna radiation capacity. The greater the antenna's ability to resist radiation, the more efficient it becomes at transmitting radiation, resulting in a stronger radiation output. Where,  $\eta_A$  for antenna efficiency,  $P_i$  for input efficiency,  $P_1$  for ohmic loss, and  $P_\Sigma$  for radiation efficiency.

$$\eta_A = \frac{P_\Sigma}{P_i} = \frac{P_\Sigma}{P_\Sigma + P_1} \quad (5)$$

### 2.2.2 Input impedance to compare the efficiency of an antenna efficiency

A good match between the antenna and the feed line is achieved when the input impedance of the antenna is the same as the characteristic impedance of the feed line. The antenna has reached its peak

power output at this moment. The antenna efficiency has also reached the highest. Fig.3 shows the line standing waves on the antenna feed line. Where  $VSWR$  is the voltage standing wave ratio,  $\Gamma$  is the reflection coefficient,  $Z_{in}$  is the input impedance,  $Z_0$  is the characteristic impedance, and  $L_r$  is the reflection loss.

$$VSWR = \frac{1 + |\Gamma|}{1 - |\Gamma|} \quad (6)$$

$$L_r = -20 \lg |\Gamma| \quad (7)$$

$$Z_{in} = Z_0 \frac{1 + \Gamma}{1 - \Gamma} \quad (8)$$

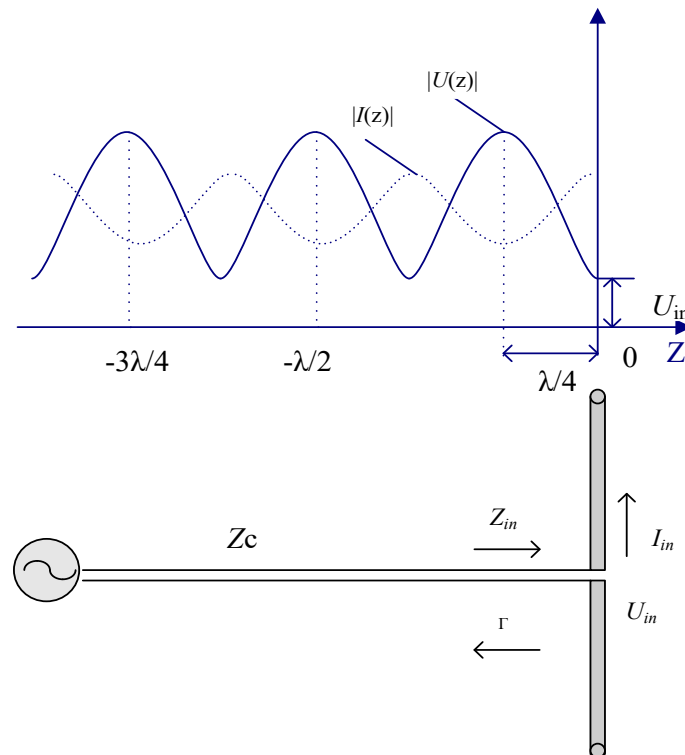


Figure 3: Line standing waves on the antenna feed line

A standing wave ratio of 1 is achieved when there is no reflection at the point of measurement. The antenna input impedance is equal to the characteristics of the feed line. The antenna radiation efficiency is also the highest.

### 2.2.3 Effects of effective length on the ability of antenna radiation

Effective length is to maintain the actual antenna maximum radiation direction of the field strength value of the conditions, assuming that the antenna current distribution is for a uniform distribution of the equivalent length of the antenna. The greater the effective length, the higher the potential for radiation power in the antenna. Take the length of the 1 symmetrical oscillator antenna can be calculated according to the following formula to obtain the effective length.

$$h_e = \frac{1}{I_0} \int_{-l}^l I_M \sin \beta(l \mp z) dz = \frac{\lambda}{\pi} \tan \frac{\beta l}{2} \quad (9)$$

$h_e$  is the effective length of the antenna,  $I_0$  is the input point current,  $I_M$  is the wave web point current and  $\beta$  is the wave number.

### 2.2.4 Effect of the effective reception area on the ability of the antenna to receive radio waves

The maximum receivable power  $P_{RM}$  of the antenna is proportional to the real power  $S_i$  of the incoming wave, and the scale factor  $A_e$  has an area dimension. The antenna's operational zone is

commonly referred to as the effective area. For a current element of length  $l$ , when the incoming electric field strength is  $E_i$ . As shown in Fig.4.

$$A_e = \frac{(E_i l)^2}{8 \times 80 \pi^2 (l / \lambda)^2 \times E_i^2 / 240 \pi} = \frac{3}{8 \pi} \lambda^2 \quad (10)$$

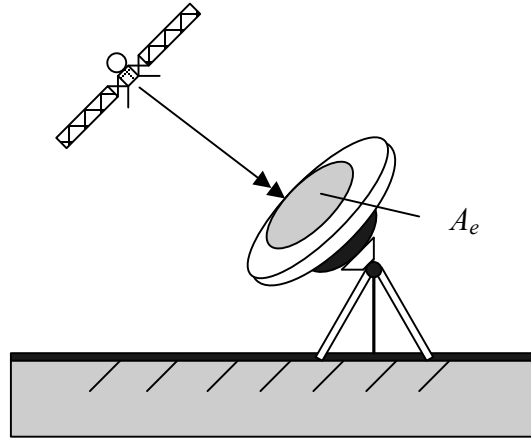


Figure 4: Effective area of the antenna

The antenna's radiation capability becomes stronger as the aperture area increases, which in turn happens when the wavelength of the antenna is larger and the received power is greater.

### 2.2.5 How antenna performance is affected by the temperature of the noise produced by the antenna

In addition to the desired signal, the surrounding noise signal is also picked up by the receiving antenna. By examining the temperature of the noise, one can gain insight into the nature of the received noise.  $T_A$  is the antenna noise temperature,  $T_a$  is the noise power equivalent of the antenna to the noise temperature at the receiver input,  $T_o$  is the actual feed line temperature and  $L_F$  is the feed line loss factor. As shown in Fig.5.

$$T_a = \frac{T_A}{L_F} + T_o \left( 1 - \frac{1}{L_F} \right) \quad (11)$$

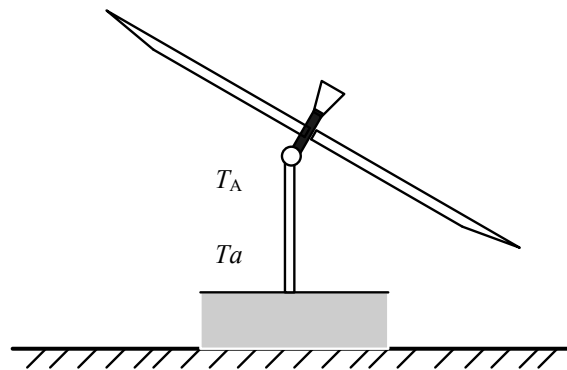


Figure 5: Antenna noise temperature concept

## 3. Model construction and analysis of results

### 3.1 Model definition

The antenna model built in this paper consists of a PTEF antenna block, a shorting sheath for impedance matching, a strip feed strip, a collector port, and a PEC ground plane, as shown in Fig.6. The PTEF antenna body is a rectangular body with a width of 15.9mm, a depth of 10mm and a height of 4mm. The two strip feed strips are a rectangular strip in the  $xz$  plane at 45mm offset from the  $y$ -axis and a

rectangular strip in the yz plane with a width of 2mm and a height of 5mm. The air domain is for a sphere with a thickness of 20mm and a radius of 100mm. In this paper, the frequency range is set to 2.10GHz, to 2.16GHz with a step size of 2.5MHz.

The housing of the phone is constructed from RF non-destructive acrylonitrile butadiene styrene material and the ABS material is set to a material property of relative magnetic permeability of 1, electrical conductivity of 0 and relative dielectric constant of 2.1. The touch display at the front of the housing uses a combination of glass with a relative magnetic permeability of 1, the electrical conductivity of  $1e-14S/m$ , a relative permittivity of 4.2, a thermal conductivity of  $1.4 [W/(m^*K)]$  and a constant pressure heat capacity of  $730 [J/(kg^*K)]$  and silicon with a relative magnetic permeability of 1, the electrical conductivity of  $1e-12S/m$  and a relative permittivity of 11.7 as a substrate. The interior of the housing is provided with a grounded FR4 circuit board with a relative permeability of 1, a conductivity of  $0.004S/m$ , a relative permittivity of 4.5, a thermal conductivity of  $0.3 [W/(m^*K)]$ , a constant pressure heat capacity of  $1369 [J/(kg^*K)]$  and a density of  $1900 [kg/m^3]$ . the FR4 circuit board has a PIFA antenna block with a relative permeability of the outside of the telephone housing is filled with an air domain where the air is set with material properties of relative permeability of 1, relative permittivity of 1, electrical conductivity of 0 and specific heat rate of 1.4. The air domain is surrounded by a perfectly matched layer of PML with a scale factor of 1 and a scale curvature parameter of 1. The PML absorbs all radiation emitted by the antenna.

In this paper, the mesh partitioning is based on the finite element method, where the area to be solved is partitioned into a finite collection of triangular or rectangular cells. For the calculation of the mobile phone model, a high degree of accuracy is required, so we need to partition the mobile phone model into refined cells, but while pursuing accuracy, we also need to pay attention to the size of the problem, i.e. the complexity of the operation, so we coarsen the partitioning of the air domain so that it is partitioned into less dense mesh cells in the curved part. At the same time, we need to satisfy the following boundary conditions:

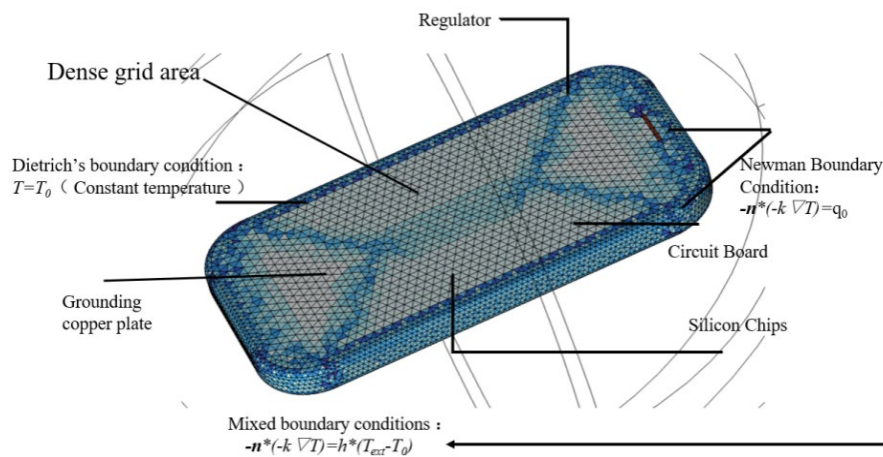


Figure 6: Geometric model and mesh sectioning of mobile communication equipment antenna structure

### 3.2 Simulation Results and Analysis

This paper presents a simulation study on the optimization of the tuning performance of PIFA antennas for multi-band applications. Taking mobile communication equipment as the research object, the simulation model of PIFA applied to mobile communication equipment is established, and the antenna tuning characteristics are used to investigate the spatial electric field distribution, far-field radiation gain characteristics and S-parameter characteristics of the PIFA structure antenna excitation in the AWS band range, and the capability of wireless communication is analysed based on the simulation results, to achieve the PIFA structure for AWS band frequency and antenna tuning characteristics to meet the current functional requirements of mobile communication devices. The spatial electric field distribution of PIFA excitation at different frequencies is shown in Fig.7.

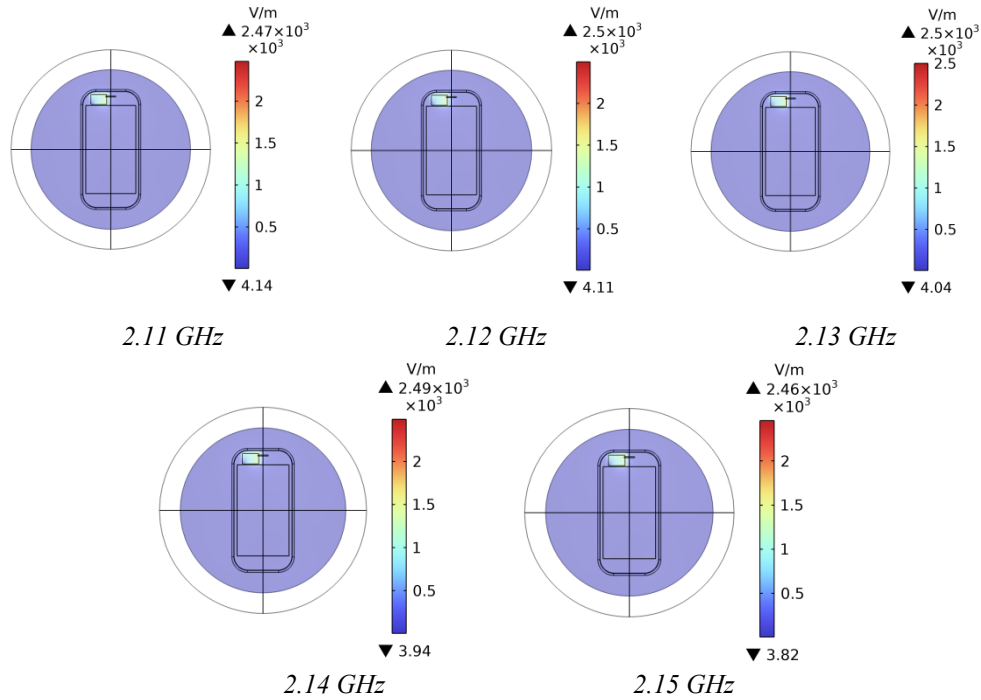


Figure 7: Electric field distribution in the PIFA excitation space at different frequencies

Different frequency PIFA two-dimensional far-field gain graph as shown in Fig.8, from the graph analysis can be seen, in the range of  $10^\circ$  to  $80^\circ$ , the antenna's far-field gain is strong, radiation intensity, high received power, while in the range of  $170^\circ$  to  $190^\circ$  and  $260^\circ$  to  $280^\circ$  range far-field gain is very weak, the radiation intensity is very small, almost cannot receive the signal. From 2.10GHz and 2.1325GHz far-field gain curve comparison can be seen, in 2.1325GHz frequency, the antenna far-field gain is stronger, radiation ability is stronger, as mobile phone antenna frequency is more in line with the current mobile communication equipment function requirements.

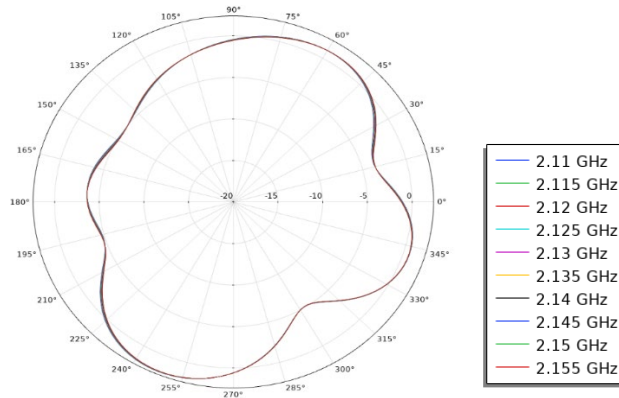


Figure 8: PIFA 2D far-field gain diagram at different frequencies

From the S-parameter variation curve with the operating frequency of the PIFA antenna in Fig.9, it can be seen that the S11 parameter is below -9.5dB in the frequency range of 2.10 GHz to 2.16 GHz. The general industry requirement is that the S11 parameter is below -13.5dB, so it shows that the antenna structure model built in this paper meets the requirement in the frequency range of 2.12GHz to 2.147GHz, and reaches the lowest value at 2.1325GHz when the impedance matching of the antenna reaches the best, the reflected energy of the antenna itself reaches the minimum, and the transmitting efficiency of the antenna reaches the highest.



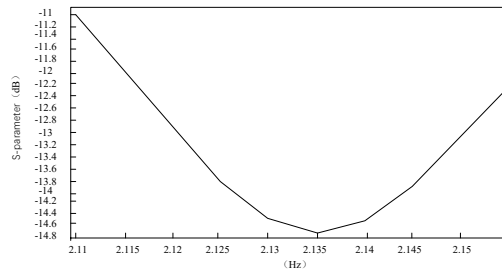


Figure 9: S-parameter characteristic curve with operating frequency

#### 4. Conclusion

The technical approach of this paper is to analyze whether the impedance matching characteristics, spatial radiation distribution and antenna tuning characteristics of PIFA antennas can meet the functional requirements of current mobile communication devices at different frequencies by building specific models of PIFA antennas under certain boundary conditions and combining the resulting S-parameter images and far-field radiation gain images in the frequency range from 2.10 GHz to 2.16 GHz. The results are as follows through experimental simulations, the following conclusions are obtained:

- (1) The functional requirements of current mobile communication equipment are met in the frequency range of 2.12 GHz to 2.147 GHz.
- (2) At 2.1325GHz, the impedance matching of the antenna is the best, the return loss of the antenna is the smallest, and the transmitting efficiency of the antenna is the highest, which is the most suitable as the antenna tuning frequency in the frequency band range studied in the experiment.
- (3) In the mobile phone antenna model, the antenna radiates the highest frequency and receives the signal most easily in the directional angle range of  $10^{\circ}$  to  $80^{\circ}$ .

#### References

- [1] Xian Richang, Fan Huifang, Li Fei, et al. Fault diagnosis of power transformers based on improved GSA-SVM model [J]. *Intelligent Power*, 2022, 50(6): 50-56.
- [2] Ma Xueqin. Analysis and design of low-profile miniaturized communication antenna [D]. Xi'an University of Electronic Science and Technology, 2022.
- [3] Chen Qixuan, Hong Tao, Hu Wei et al. Design of PIFA antenna for SAR reduction based on ring parasitic branch loading [C]//Chinese Institute of Electronics. *Proceedings of the 2021 Annual National Antenna Conference*, 2021: 2264-2267.
- [4] Zhang Hao. Research on broadband impedance matching and high stability phase centre antenna technology [D]. Xi'an University of Electronic Science and Technology, 2021.
- [5] Cai Jiaqi, Zhang Jindong, Wu W. Compact broadband PIFA antenna loaded with inverted L-shaped steps [J]. *Journal of Microwave*, 2019, 35(S1): 25-28.
- [6] Xia Yiping. Inverted F antenna for mobile terminals and its miniaturization [D]. Xi'an University of Electronic Science and Technology, 2019.
- [7] Qin Xianghong. Design of PIFA antenna with an open branch with filtering effect [J]. *Digital Communication World*, 2022(10): 14-17.
- [8] Wang B., Cao W. K., Ma W. Y., Li D. H.. Design of dual-band circularly polarized common aperture antenna based on structural multiplexing [J]. *Microwave Journal*, 2023, 39(01): 8-12.
- [9] Su Wei. Optimal design of an antenna reflector structure based on finite elements [J]. *Mechatronics Information*, 2022(12): 40-43.
- [10] Fei Qiuxian. Study on CDMA455, LTE PIFA antenna and its parasitic structure for small base station [C]. // Chinese Institute of Electronics. *Proceedings of the 2021 Annual National Antenna Conference*. 2021: 248-253.
- [11] Kumar R, Suraj P. Antipodal vivaldi antenna for UWB communication with metamaterials design, modelling and analysis of antipodal vivaldi antenna with EBG structures[C]//International Conference on Inventive Systems & Control.2017:1-5.DOI:10.1109/ICISC.2017.8068742.
- [12] Wang ZG, Yu Miao, Wang Jianbo, Lu J. Design and study of the decoupling structure of microstrip patch antenna based on 5G communication band [J]. *Journal of Changchun University of Technology (Natural Science Edition)*, 2020, 43(02): 38-42+47.